Inhibiting Lysyl Oxidases prevents pathologic cartilage calcification

Ilaria Bernabei [a], Elodie Faure [a], Mario Romani [b], Julien Wegrzyn [c], Jürgen Brinckmann [d], Véronique Chobaz [a], Alexander So [a], Thomas Hugle [a], Nathalie Busso [a], Sonia Nasi [a,*]

[a] *Service of Rheumatology, Department of Musculoskeletal Medicine, Lausanne University Hospital and University of Lausanne; Lausanne, Switzerland*
[b] *Aging and Bone Metabolism Laboratory, Service of Geriatric Medicine & Geriatric Rehabilitation, Department of Medicine, Lausanne University Hospital and University of Lausanne; Lausanne, Switzerland*
[c] *Department of Orthopedic Surgery, Lausanne University Hospital and University of Lausanne, Lausanne, Switzerland*
[d] *Department of Dermatology and Institute of Virology and Cell Biology, University of Lübeck, Lübeck, Germany*

A B S T R A C T

Lysyl oxidases (LOX(L)) are enzymes that catalyze the formation of cross-links in collagen and elastin fibers during physiologic calcification of bone. However, it remains unknown whether they may promote pathologic calcification of articular cartilage, an important hallmark of debilitating arthropathies. Here, we have studied the possible roles of LOX(L) in cartilage calcification, related and not related to their cross-linking activity. We first demonstrated that inhibition of LOX(L) by β-aminoproprionitrile (BAPN) significantly reduced calcification in murine and human chondrocytes, and in joint of meniscectomized mice. These BAPN's effects on calcification were accounted for by different LOX(L) roles. Firstly, reduced LOX(L)-mediated extracellular matrix cross-links downregulated *Anx5*, *Pit1* and *Pit2* calcification genes. Secondly, BAPN reduced collagen fibrotic markers *Col1* and *Col3*. Additionally, LOX(L) inhibition blocked chondrocytes hypertrophic differentiation (*Runx2* and COL10), pro-inflammatory IL-6 release and reactive oxygen species (ROS) production, all triggers of chondrocyte calcification. Through unbiased transcriptomic analysis we confirmed a positive correlation between LOX(L) genes and genes for calcification, hypertrophy and extracellular matrix catabolism. This association was conserved throughout species (mouse, human) and tissues that can undergo pathologic calcification (kidney, arteries, skin). Overall, LOX(L) play a critical role in the process of chondrocyte calcification and may be therapeutic targets to treat cartilage calcification in arthropathies.

1. Introduction

Lysyl oxidases (LOX(L)) constitute a family of enzymes, including lysyl oxidase (LOX) itself and four lysyl oxidase-like proteins (LOXL1, 2, 3, 4) [1]. These enzymes play an important role in extracellular matrix (ECM) maturation and integrity, through cross-linking collagen and elastin fibres. Beyond their cross-linking function, the LOX(L) family is involved in various biological processes. Intriguingly, extracellular LOX can re-enter cells and exerts intracellular functions. Indeed, LOX has been identified in the nucleus, where it acts as transcription regulator for elastin and for the fibrotic collagen type III (*COL3*) [2,3]. Furthermore, cytosolic LOX has been implicated in inflammation in scleroderma, via upregulation of the IL-6 transcription factor [4]. LOX overexpression has also been associated with oxidative stress, as it produces H_2O_2 as a by-product of its activity [5].

Pathologic calcification refers to the deposition of calcium-containing crystals in tissues that tipically do not calcify such as cartilage, vessels and skin [6]. Cartilage calcification is a hallmark of disabling arthropathies, such as osteoarthritis (OA). Remarkably, calcification is detected in up to 100% of OA cartilages obtained from knee or hip joint replacement [7] and it is increasingly considered as an etiologic factor rather than a bystander in OA. Indeed, cartilage calcification correlated with histological cartilage damage and radiographic disease severity [7,8]. Accordingly, inhibiting calcification has shown to be protective against cartilage damage in mouse models [9].

Cartilage calcification results from the formation and deposition of calcium-containing crystals, such as basic calcium phosphate (BCP) and calcium pyrophosphate dihydrate (CPPD), by chondrocytes [10]. The intricate calcification machinery involves enzymes and channels that regulate PP_i, P_i and Ca^{2+} levels: pyrophosphatase/phosphodiesterase 1 (ENPP1), cell-associated ankylosis protein (ANK), alkaline phosphatase (ALP), Na/Pi cotransporters (PIT1/2), and Annexin V channel (ANXV).

Several mechanisms trigger this calcification machinery. The first one is differentiation of quiescent chondrocytes into hypertrophic calcifying chondrocytes, expressing collagen type X (COL10) and runt related transcription factor 2 (*Runx2*) [11–13]. Additional enhancers of the chondrocytes hypertrophic differentiation and calcification process are inflammation (in particular, interleukin-6 (IL-6)) [14] and oxidative stress (reactive oxygen species (ROS) production) [15]. Once formed, crystals can amplify these detrimental effects [9,14,16], ultimately leading to cartilage damage through the activation of matrix-degrading enzymes (metalloproteases (MMP3, −9, −13) and aggrecanases (ADAMTS4, −5) [8]).

So far, the role of LOX(L) in cartilage pathology remains unclear and has yielded controversial results. On one hand, LOX overexpression correlated with more severe damage in human cartilage, and transgenic LOX (TgLOX) mice had increased susceptibility to develop experimental OA [17]. On the other hand, LOX and LOXL2 overexpression enhanced cartilage cross-links and tensile properties, thus representing a potential approach in regenerative medicine [18]. Finally, LOXL2 upregulation protected against IL-1β-induced metalloproteases in human chondrocytes [19] and alleviated pain while improving functional parameters in OA mice [20]. However, all these studies have not addressed the question of whether LOX(L) dysregulation may impact cartilage calcification.

In the present work we aimed to elucidate whether LOX(L) dysregulation plays a role in cartilage calcification and to detail the mechanisms underlying its actions.

2. Results

2.1. LOX(L) inhibition reduces chondrocytes calcification

We found that primary murine chondrocytes express all *Lox(l)* genes (*Lox, Lox1, Loxl2, Loxl3, Loxl4*), *Lox* and *Loxl2* being the predominant isoforms (Fig. S1). Nevertheless, in the current work we focused on the involvement of the whole LOX(L) family in calcification. The study of each of the four isoforms was outside the scope of our manuscript and will be addressed in upcoming investigations. Here, we demonstrated that LOX(L) activity was significantly induced by two different calcification media (CM: high phosphate medium (HPM) or secondary calci-protein particles (CPP) [21]) compared to control medium (Nt) (Fig. 1a). To confirm these data, we measured, by HPLC, LOX(L) generated cross-links in chondrocytes cultured in CM. We found a trend toward increased of DHLNL (hydroxylysine-aldehyde derived cross-link) and HLNL (lysine- or hydroxylysine-aldehyde derived cross-link) in cells cultured in CM compared to Nt, although not significant (DHLNL: Nt=100.0% ± 5.5% CM=103.4% ± 4.1%, HLNL: Nt=100.0% ± 5.8% CM=104.9% ± 9.5%; values represent mean ± SD of four independent experiments). LOX(L) activity was similarly induced by pre-formed calcium-containing crystals (hydroxyapatite HA; octacalcium phosphate OCP; carbonated apatite CA) (Fig. 1a). Both CM and crystals had no cytotoxic effect on chondrocytes (Fig. S2a). Conversely, pan-inhibition of LOX(L) by β-aminoproprionitrile (BAPN) led to a striking reduction of calcium-containing crystal formation in chondrocytes, as shown by Alizarin red staining (Fig. 1b, red spots and graphs). This occurred in both 2D monolayer culture (Fig. 1b, upper panel) as well as in 3D micromasses (Fig. 1b, lower panel), which better reflects the complexity of cartilage extracellular matrix. No cytotoxic effect was revealed by BAPN treatment, as demonstrated by LDH measurement (Fig. S2b).

To explain the BAPN anti-calcification effect, we investigated the expression of calcification genes and found downregulation of *Anx5, Enpp1, Pit1, Pit2* (Fig. 1c). While *Alpl* gene expression was not modulated by BAPN, ALP activity was significantly reduced (Fig. 1d). This discrepancy can be explained by the fact that *Alpl* gene expression was measured at the same experimental time than ALP activity, therefore we likely missed the modulation of the gene.

Finally, we confirmed the anti-calcifying effect of LOX(L) inhibition on human chondrocytes. Indeed, cells from cartilages of four OA patients and treated with BAPN displayed less calcium-containing crystal production (Fig. 1e), without any cytotoxic effect as measured by LDH (Fig. S2c). Overall, LOX(L) is upregulated during chondrocyte calcification and inhibiting its enzymatic activity reduced calcification.

2.2. LOX(L) role in matrix cross-linking sustains chondrocyte calcification

We first investigated if the role of LOX(L) in calcification was related to matrix cross-linking. We generated chondrocytes extracellular matrices having different degrees of cross-links by treating these cells with different concentrations of BAPN (Fig. 2a, left panel). No BAPN concentration demonstrated cytotoxic effect (Fig. S2d). We proved by HPLC analysis, that BAPN decreased in a dose-dependent manner both total (Fig. 2a, left graph) and individual matrices cross-links (Fig. S3a). Moreover, matrices obtained after cell lysis and removal did not show any sign of calcification (Fig. S3b). In Step 2, new chondrocytes were plated on the matrices and cultured in CM (Fig. 2a, middle panel). After 3 days, Alizarin red staining revealed that the degree of matrix cross-links positively correlated with chondrocyte calcification (Fig. 2a, right panel and graph). Additionally, expression of calcification genes (*Anx5, Pit1* and *Pit2*) decreased proportionally to diminished cross-links in these cells (Fig. 2b).

2.3. LOX(L) roles in hypertrophy, fibrosis, inflammation, and oxidative stress sustains chondrocyte calcification

We further explored if other LOX(L) roles unrelated to their cross-linking activity contributed to calcification. Firstly, we studied if transcription factors and collagens involved in chondrocyte hypertrophy were affected. While CM down-regulated early differentiation chondrogenic markers (*Sox9, Col2*) and upregulated hypertrophic markers (*Runx2, Col10*), BAPN reverted these effects (Fig. 3a, left graph). Immunohistochemical analysis on micromasses confirmed significantly decreased collagen type X (COL10) by BAPN at the protein level (Fig. 3a, pictures and right graph). Next, the effect of BAPN on synthesis of fibrotic collagens type I (*Col1*) and III (*Col3*) was evaluated. There was strong induction of both collagen genes by CM, which was reduced by BAPN treatment (Fig. 3b, left graph). COL1 and COL3 protein expression were slightly reduced in BAPN-treated micromasses, although not significantly (Fig. 3b, pictures and right graphs). We then investigated other possible mechanisms by which LOX(L) inhibition could protect against chondrocyte calcification, such as inflammation and oxidative stress. We found that CM induced IL-6 in chondrocytes, both at the mRNA and at the protein level, while BAPN significantly reverted this induction (Fig. 3c). A trend towards decreased IL-6 by BAPN was also found in human chondrocytes (Fig. S4). Finally, we demonstrated that calcification stimuli triggered mitochondrial (MitoSOX) and cellular (DHE) ROS production, while BAPN was protective (Fig. 3d).

2.4. LOX(L) inhibition protects against calcification in joints of meniscectomized mice

Given the beneficial effects of LOX(L) inhibition observed in vitro, we tested BAPN in a murine model of joint calcification in vivo [14]. No mice died during treatment, nor did they show signs of toxicity, loss of weight or discomfort. First, we confirmed an inhibitory effect by BAPN on LOX(L) activity in mice sera at day of sacrifice (Fig. 4a). Second, two months after surgery, knees of BAPN-treated mice displayed decreased newly formed periarticular calcific deposits, compared to knees of PBS-treated mice (Fig. 4b, green areas). Indeed, MicroCT-scan quantitative analysis revealed significant decrease in volume and crystal content of these calcified deposits (Fig. 4c). To rule out any unwanted effect of BAPN on already existing mineralized knee structures, we first
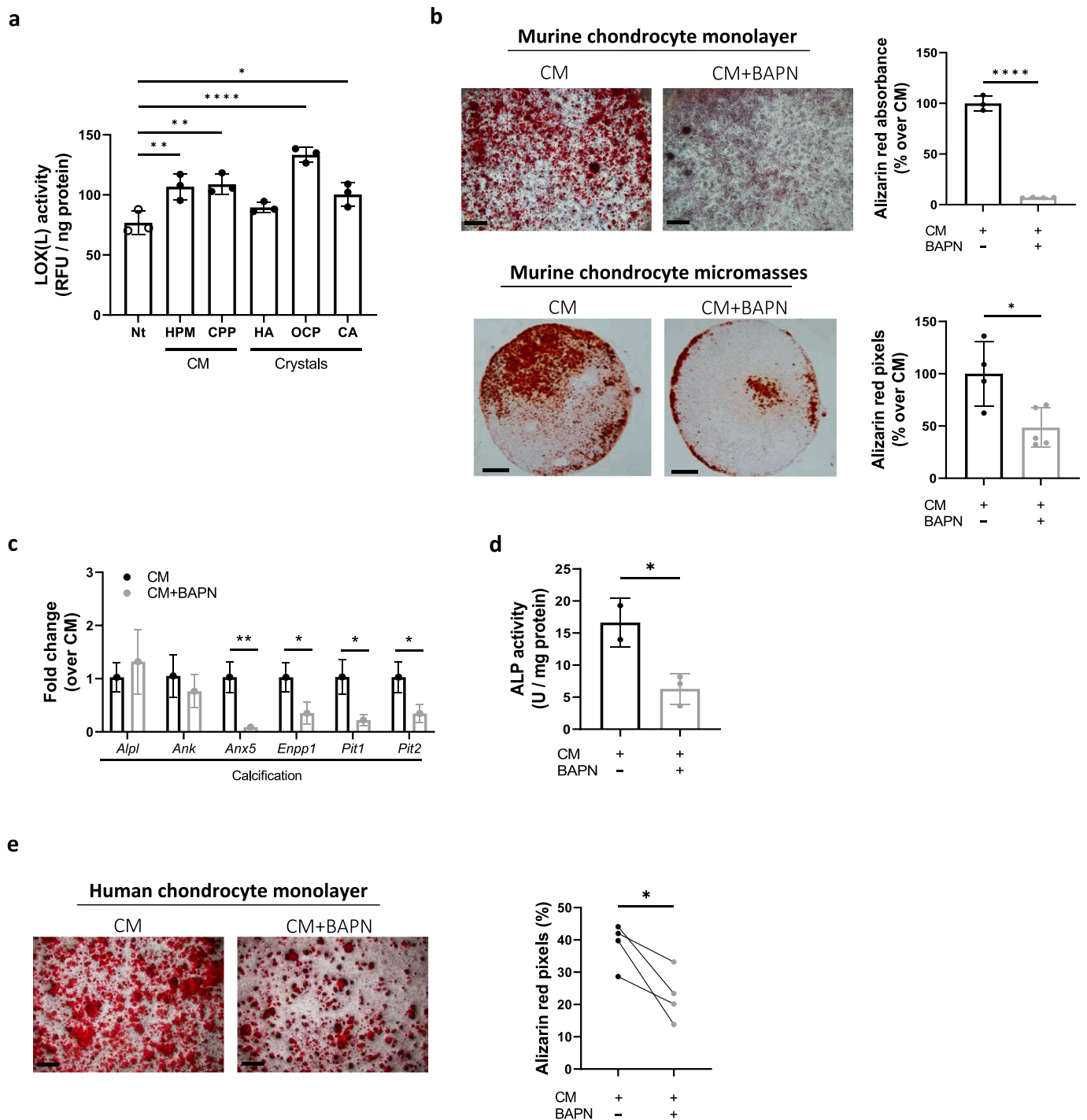
Fig. 1. LOX(L) inhibition is beneficial against chondrocytes calcification. (A) LOX(L) activity in murine chondrocytes cultured for 24 h in Nt medium, in CM media (HPM, CPP) or in presence of 500 µg/ml of crystals (HA, OCP, CA). One-way ANOVA (n = 3). (**B**) Alizarin red staining and quantification in murine chondrocyte monolayers and micromasses cultured for 14 days in CM, treated or not with 500 µM BAPN. Graphs represent Alizarin red quantification in cell monolayers, expressed in % over CM cells, unpaired t-test (n = 3–4) or in micromasses, expressed in % over CM micromasses, unpaired t-test (n = 4–5). (**C**) qRT-PCR analysis of the indicated genes in murine chondrocytes cultured for 7 days in CM, treated or not with BAPN. Expression was normalized over CM. Two-way ANOVA (n = 3). (**D**) ALP activity in murine chondrocytes lysates cultured for 7 days in CM, treated or not with BAPN. Unpaired t-test (n = 3). All results represent mean ± SD. (**E**) Alizarin red staining and quantification in human OA chondrocytes cultured for 14 days in CM, treated or not with BAPN. Pictures show one representative patient. Graph represents Alizarin red quantification in chondrocytes from OA patients, expressed in % of red pixels over total amount. Paired t-test (n = 4). *p < 0.05, * * p < 0.01, * ** * p < 0.0001. Scale bars 500 µm.

a
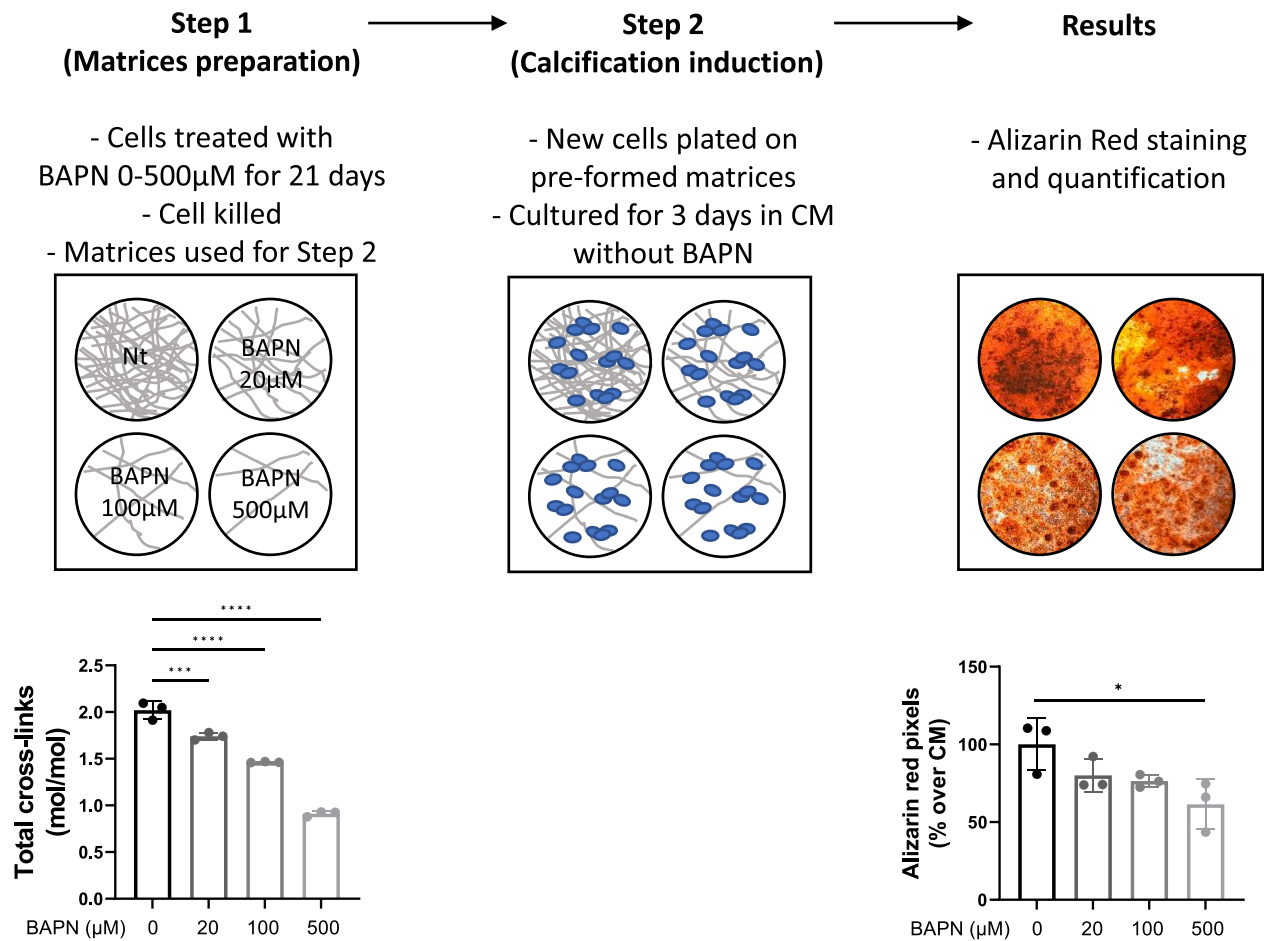
b
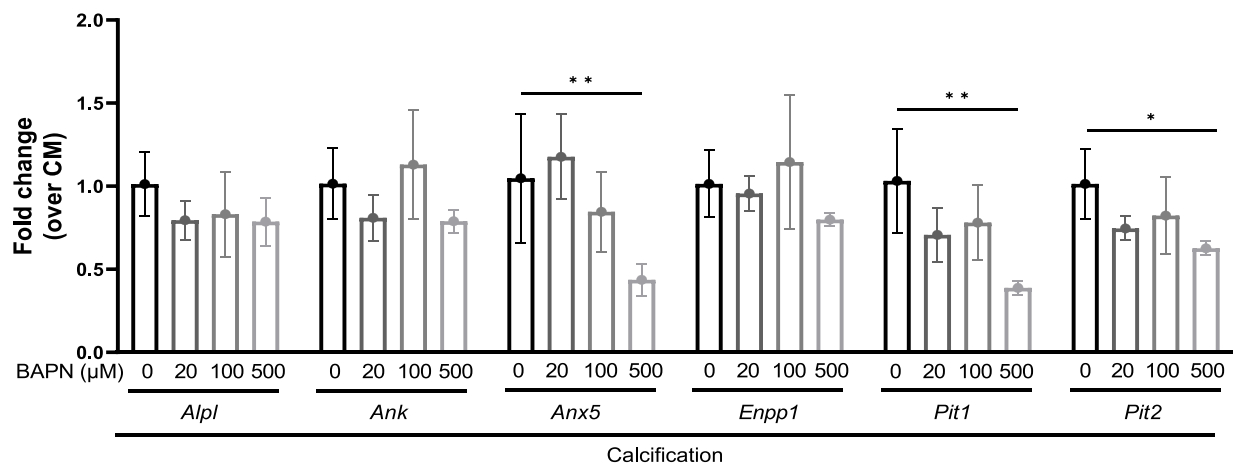
Fig. 2. LOX(L) role in matrix cross-linking sustains chondrocyte calcification. (A) In Step 1, we cultured primary murine chondrocytes in non-calcifying medium for 21 days in presence of increasing concentrations of BAPN (0–500 μM). Total cross-links were measured in these matrices, and results are shown in the left graph. One-way ANOVA (n = 3). In Step 2, following removal of chondrocytes, we cultured a new set of chondrocytes on pre-formed matrices for 3 days in CM. Finally, we performed Alizarin red staining and quantification to evaluate calcification, right panel and graph. One-way ANOVA (n = 3). (B) qRT-PCR analysis of the indicated genes in murine chondrocytes cultured for 3 days in CM on pre-formed matrices. Expression was normalized over Nt. Two-way ANOVA (n = 3). All results represent mean ± SD. *p < 0.05, * * p < 0.01, * ** p < 0.001, * ** * p < 0.0001.
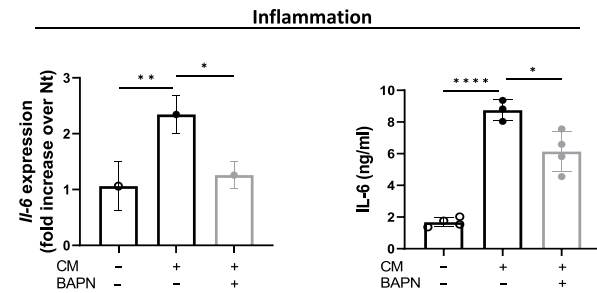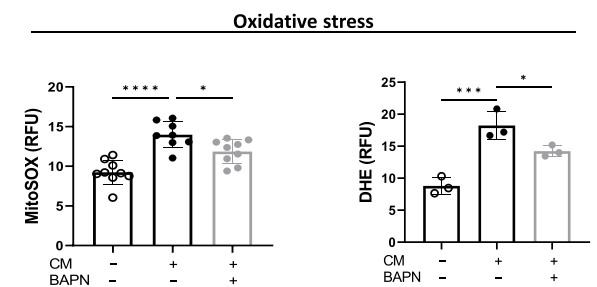
a

Hypertrophy

b

Fibrosis

c

Inflammation

d
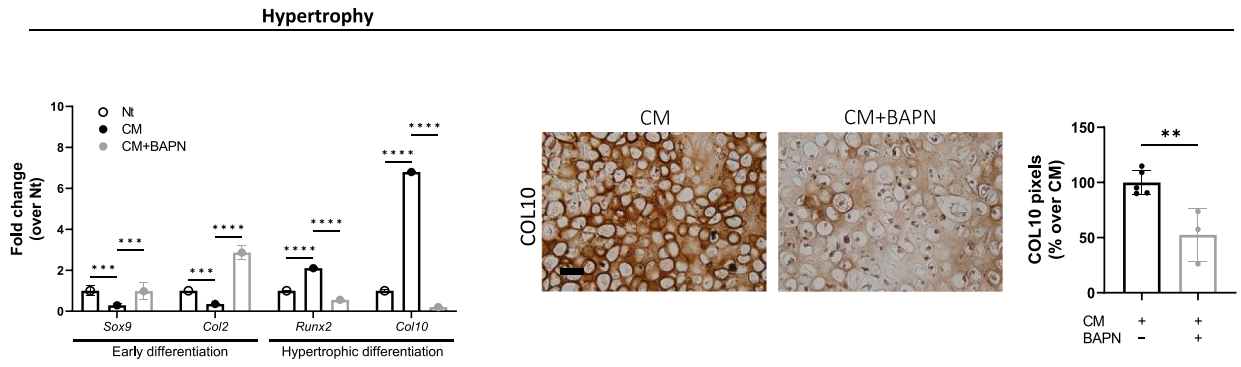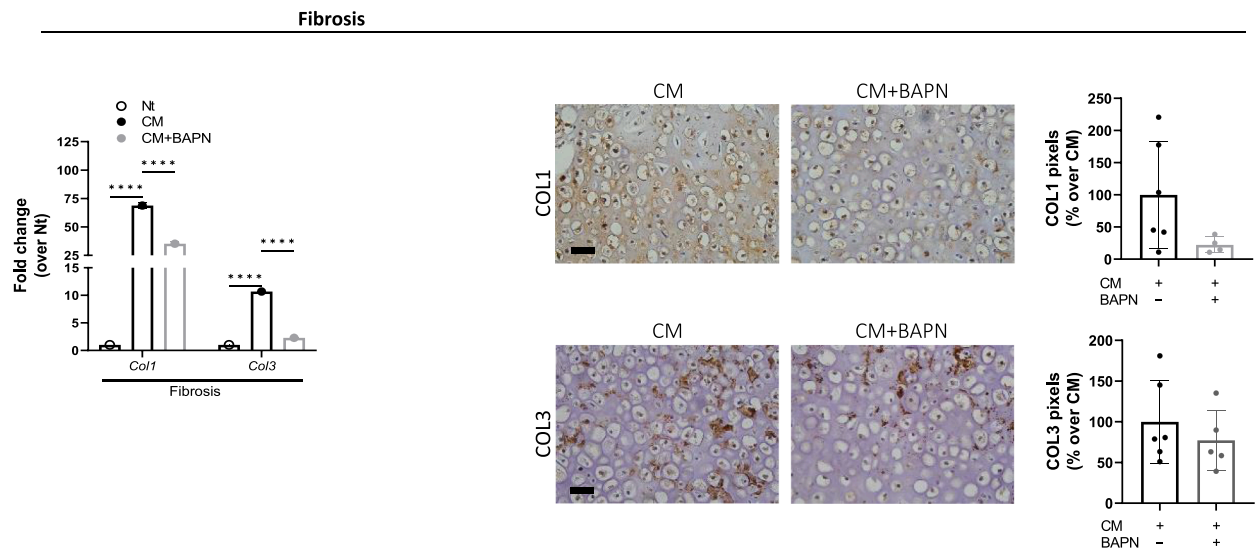
Oxidative stress

(caption on next page)

Fig. 3. LOX(L) roles in hypertrophy, fibrosis, inflammation, and oxidative stress sustains chondrocyte calcification. (A) qRT-PCR analysis of the indicated genes in murine chondrocytes cultured for 7 days in Nt medium or in CM, treated or not with BAPN. Expression was normalized over Nt. Two-way ANOVA (n = 3). Pictures show IHC for COL10 in micromasses cultured for 14 days in CM, treated or not with BAPN. Graph represents COL10 positive pixels quantification, expressed in % over CM. Unpaired t-test (n = 3–5). Scale bars 500 μm. (B) qRT-PCR analysis of the indicated genes in murine chondrocytes cultured for 7 days in Nt medium or in CM, treated or not with 500 μM BAPN. Expression was normalized over Nt. Two-way ANOVA (n = 3). Pictures show IHC for COL1 and COL3 in micromasses cultured for 14 days in CM, treated or not with BAPN. Graphs represent COL1 and COL3 positive pixels quantification, expressed in % over CM. Scale bars 20 μm. Unpaired t-test (n = 4–6). (C) IL-6 by qRT-PCR and ELISA in chondrocytes cultured for 7 or 14 days in Nt medium or CM, treated or not with BAPN. Expression was normalized over Nt. One-way ANOVA (n = 3–4). (D) Mitochondrial (MitoSOX) and cellular (DHE) ROS measured in chondrocytes cultured for 1 h in Nt medium or CM, treated or not with BAPN. One-way ANOVA (n = 3–9). All results represent mean ± SD. *p < 0.05, * * p < 0.01, * ** p < 0.001, * ** * p < 0.0001.

---

analysed tibial subchondral trabecular bone (Fig. 4d, red lines). Neither bone mineral density (BMD) nor trabecular thickness (Tb.Th) were impacted by LOX(L) inhibition (Fig. 4e). Additional structures such as medial posterior meniscus, lateral meniscus, and rotula were not impacted by BAPN (Fig. S5).

2.5. LOX(L) module positively correlates with calcification-related modules in an unbiased transcriptomic analysis

In an unbiased large-scale transcriptomic analysis, we identified which gene modules (= clusters) correlated with the LOX(L) genes module. Module-module association analysis was performed on a pool of 152 human datasets of kidney, brain, skin, artery, muscle, and soft tissues, using the genetic toolkit GeneBridge [22]. Results indicated that LOX(L) genes module, defined as collagen fibril organization module, had a strong positive correlation with calcification-related modules (i.e. calcification, hypertrophy and catabolic enzymes genes) (Fig. 5a) (for individual module identifiers and module-module association score (MMAS) see Table S1). This association was largely conserved when tissues were analyzed independently (Fig. 5b, for individual module identifiers and MMAS see Tables S2-7). A similar positive association was observed in a pool of 71 mouse datasets of kidney, brain, skin, and muscle, indicating a cross-species conservation of this mechanism (Fig. 5c) (for individual module identifiers and MMAS see Table S8). Altogether these data suggest that our results characterizing a link between LOX(L) activity and calcification in cartilage could be relevant also for other calcification-prone tissues, potentially expanding our findings to a plethora of pathologies including vascular, brain, kidney, skin, and muscle calcification.

3. Discussion

Pathologic cartilage calcification stands as a major contributor to cartilage degradation, and currently, there are no available disease-modifying treatments. Our study establishes a deleterious role of LOX (L) in pathologic cartilage calcification. While it is well established that LOX(L) activity supports physiologic calcification in bone [23,24], its role in cartilage calcification has remained unexplored so far. In this work, LOX(L) activity was augmented by calcification stimuli. Conversely, LOX(L) inhibition by BAPN was protective against crystal formation in chondrocyte cultures, likely through the downregulation of calcification genes (*Anx5, Enpp1, Pit1, Pit2*) and reduction of ALP activity. We validated this protective effect of BAPN in in vitro human chondrocytes isolated from OA patients as well as in the meniscectomy murine model of joint calcification. In the latter, we observed a significant decrease in newly formed calcific deposits in knees of BAPN-treated mice, while we ruled out any adverse effect of LOX(L) inhibition on pre-existing mineralized structures, such as subchondral bone. Similar findings were previously obtained in vessels undergoing pathologic calcification, where LOX overexpression exacerbated vascular smooth muscle cells (VSMCs) calcification in vitro [25], while BAPN reduced aortic calcification in mice in vivo [26]. Notably, the involvement of LOX and LOXL2 in cartilage damage, independent of calcification, has been reported with conflicting results [17,18,20,27].

To unravel the possible mechanisms through which increased LOX (L) may promote cartilage calcification, our initial focus was on their cross-linking role. We showed that a highly cross-linked extracellular matrix sustains chondrocyte calcification, while a poorly cross-linked matrix leads to the opposite outcome. In line, increased COL1 cross-links via LOX and PLOD1 (lysyl hydroxylase 1) led to trans-differentiation of VSMCs into calcifying osteoblast-like cells [25]. Recent findings linked age-related matrix stiffening to disrupted cartilage integrity [28]. This was mediated by decreased α-Klotho, whose deficiency in zebrafish associates with cardiovascular calcification [29]. It remains to be clarified whether LOX(L) are active upstream or downstream to α-Klotho.

Matrix stiffness, a crucial regulator of tissue fibrosis [30], is closely intertwined with calcification in various tissues, including cardiovascular tissues [31], bronchial cartilage [32], and articular cartilage [33]. Two pivotal fibrotic collagens are COL1 and COL3 [30]. Extracellular LOX can translocate to the nucleus and serve as a transcription regulator of *COL3* gene [2]. In our study, LOX(L) inhibition by BAPN reversed the induction of *Col1* and *Col3* by calcification medium in chondrocytes, albeit with only a slight decrease observed at the protein level.

An additional collagen important in cartilage calcification is collagen type X. In particular, increased COL10 drives chondrocyte hypertrophy and subsequent calcium-containing crystal deposition [10]. In our study, we confirmed that BAPN suppressed chondrocyte hypertrophy (*Runx2*, COL10) triggered by calcification conditions, while simultaneously maintaining a healthy chondrogenic phenotype (*Sox9* and *Col2*). Accordingly, LOX overexpression in VSMCs was accompanied by *Runx2* upregulation and their transdifferentiation into calcifying osteoblast-like cells [25].

Recent investigations have linked LOX to inflammation in scleroderma, as it mediates nuclear translocation of c-Fos and its interaction with the *IL-6* promoter [4]. We previously established that a vicious cycle exists in chondrocytes, where IL-6 and calcification mutually amplify each another [14]. Here we demonstrated that BAPN effectively decreased the expression and secretion of IL-6 by murine and human chondrocytes cultured in calcification conditions. Consequently, we propose that LOX(L) may contribute to cartilage calcification by promoting up-modulation of IL-6.

Another important player in cartilage calcification are reactive oxygen species, including H_2O_2, $O2^-$ and OH. In chondrocytes, ROS induced hypertrophy and subsequent crystal production [15]. In turn, crystals triggered ROS in chondrocytes and macrophages [9]. In our present study, we demonstrated that BAPN lowered calcification-induced ROS. This decrease could be attributed to diminished release of H_2O_2, a byproduct of the LOX(L) catalytic cycle. Accordingly, arteries from TgLOX mice exhibited elevated vascular H_2O_2 levels while BAPN prevented oxidative stress in experimental models of hypertension [5].

Finally, by unbiased transcriptomics analysis, we uncovered evidence of a positive association between LOX(L) genes and genes involved in calcification mechanisms, spanning across species (human and mouse) and across multiple potentially calcifying tissues (kidney, artery, muscle, brain, skin and soft tissue). These bioinformatics findings strengthen our in vitro and in vivo results, emphasizing that LOX(L) are critical contributors to the induction of pathologic calcification.

The limitations of the study include: firstly, the LOX(L) activity assay we used, based on H_2O_2 detection, is sensitive to background and interferences given that H_2O_2 is produced by multiple cellular pathways.
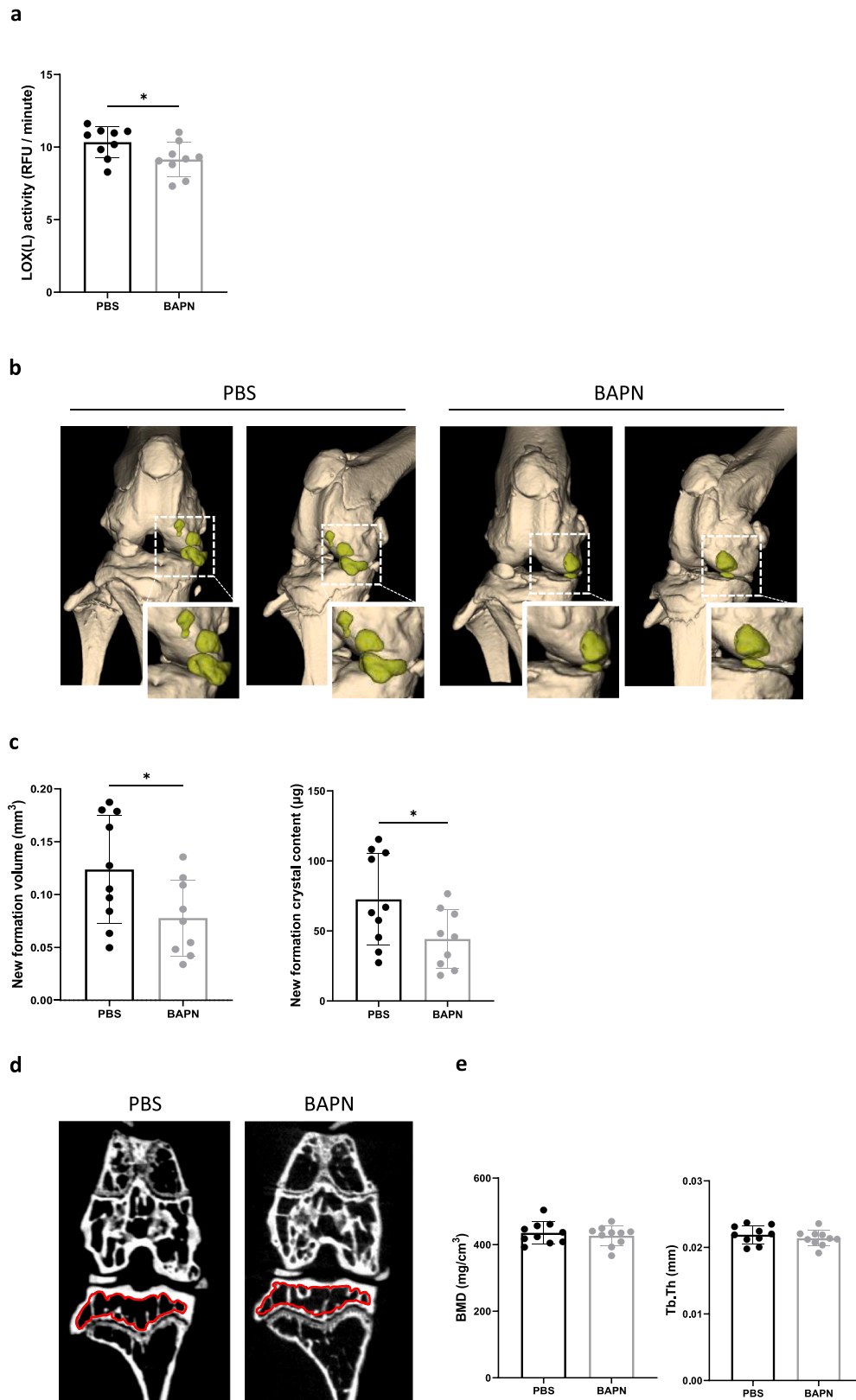
Fig. 4. LOX(L) inhibition diminished new crystal deposits in joints of meniscectomized mice (A) LOX(L) activity in sera of meniscectomized mice treated with PBS or BAPN. Unpaired t-test (n = 9). (**B**) Representative frontal and lateral 3D MicroCT scan images of knee joints from mice treated with PBS or BAPN for two months after surgery. Magnified new crystal formations in squares. (**C**) Corresponding analysis of new formations volume (bone volume in mm^3) and crystal content (µg). Unpaired t-test (n = 9–10). (**D**) Representative 2D MicroCT scan images of knee joints from PBS or BAPN treated mice. Analysed regions of tibial subchondral bone are highlighted in red. (**E**) Corresponding analysis of bone mineral density (BMD, mg/cm^3) and trabecular thickness (Tb.Th, mm). Unpaired t-test (n = 9–10). All results represent mean ± SD. * p < 0.05.
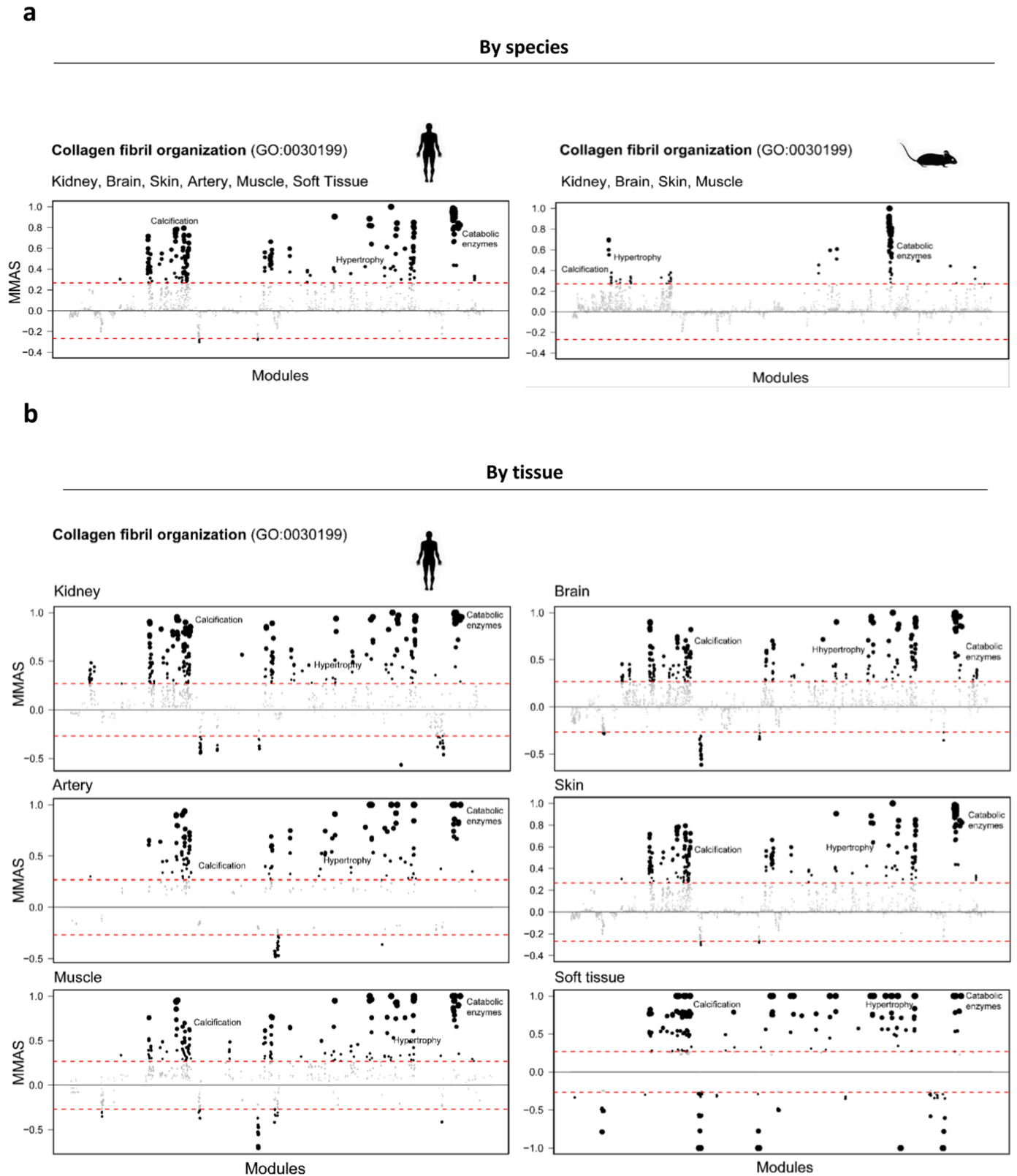
Fig. 5. LOX(L) gene module positively correlates with calcification-related modules throughout species and potentially calcifying tissues. (A) Association analysis of LOX(L) gene module (i.e. collagen fibril organization module (GO:0030199)) and calcification, hypertrophy and catabolic enzyme modules, in 152 human datasets of kidney, brain, skin, artery, muscle and soft tissues. (B) Association analysis of LOX(L) gene module (i.e. collagen fibril organization module (GO:0030199)) and calcification, hypertrophy and catabolic enzymes modules in human datasets of kidney (30 datasets), brain (73 datasets), skin (27 datasets), muscle (12 datasets), artery (6 datasets) and soft tissues (4 datasets). The threshold of significant module-module connection is indicated by the red dashed line. (C) Association analysis of LOX(L) gene module (i.e. collagen fibril organization module (GO:0030199)) and calcification, hypertrophy and catabolic enzyme modules, in 71 murine datasets of kidney, brain, skin, and muscle. MMAS = module-module association score.

Nevertheless, the assay we used is the gold standard in this field [34]. Secondly, we did not explore the specific molecular mechanisms involved in BAPN-modulated gene expression. It is likely that these effects are attributed to LOX(L) ability to regulate promoter activities and modify histones [3,4], a subject that warrants exploration in future experiments. Thirdly, the use of the pan-inhibitor BAPN did not allow for the identification of the specific LOX(L) isoform involved. Targeting the specific LOX(L) that responsible for cartilage calcification is crucial for future clinical applications to mitigate potential adverse effects, such as aortic aneurysm [35]. Ongoing studies in our laboratory are addressing specifically the role of LOX LOXL2 in cartilage calcification. Fourthly, in the bioinformatics analysis, the LOX(L) gene module (collagen fibril organization module) included not only LOX(L) genes, but also genes for matrix proteins (collagens, aggrecan, elastin), matrix growth factors (*TGFβ2*), and others. However, the online tool used did not allow the selection of specific genes outside of predefined modules. Finally, although we did not investigate the chronological sequence of events depicted in Fig. 6, based on previous findings [14,15,17,36,37] we hypothesize that a dynamic interplay exists between all these mechanisms.

In summary, the data presented in this study demonstrated that elevated LOX(L) levels and activity induce cartilage calcification through both their classical role in extracellular matrix cross-links and non-classical roles (chondrocyte hypertrophy, fibrosis, inflammation, and oxidative stress), as illustrated in Fig. 6.

In conclusion, our findings position LOX(L) as promising targets for the treatment of pathologic cartilage calcification in arthropathies. Most importantly, these insights may hold therapeutic implications for other calcifying diseases, including atherosclerosis and scleroderma.

4. Methods

4.1. Study design

This study was performed to evaluate whether LOX(L) enzymes play a role in pathologic cartilage calcification. This objective was addressed by (i) studying the effect of the LOX(L) pan-inhibitor BAPN on human and murine chondrocyte calcification, (ii) treating meniscectomized mice with BAPN, (iii) delineating the possible underlying molecular mechanisms, (iv) analyzing the association between LOX(L) and calcification-related genes in transcriptome datasets available online. For in vitro studies, sample size was determined according to previous experimental experience. Each experiment has been repeated at least twice. Primary chondrocytes isolated from newborn mice knees and primary human chondrocytes from undamaged knee cartilage of OA patients were used. Overall, no outlier was removed with respect to its deviation from the mean in any of the in vitro experiments. Exclusion criteria for real-time polymerase chain reaction included genes with Ct over 38. Exclusion criteria for micromasses included technical issues such as section overlap or detachment not allowing a proper scoring. For in vivo experiments we estimated sample size by power analysis: based on our previous studies in similar experimental settings [9,14], we expected around 50% difference in the size of cartilage calcific deposits. Considering our experimental standard deviation, analysis by post-hoc one-way ANOVA followed by bilateral one-sample t-test, an α-error of 0.05 and a power of ≥ 0.8, n = 10 mice/group was the good sample size to adopt. Mice were assigned randomly to the experimental and control groups and divided in four cages of 5 mice (two cages PBS-treated and two cages BAPN-treated). Mice allocation, data acquisition and analysis were performed in a blinded manner by two independent investigators (I.B.; V.C.). The only exception was unblinded injections of mice. Exclusion criteria before completion of the experiment encompass any major discomfort from the animals after surgery and analgesic treatment. All animals were observed by trained personnel daily and given a score according to the veterinary office to evaluate their health status. None of the animals met these criteria. The primary (new formation volume and crystal content) and secondary (subchondral bone mineral density and trabecular thickness) endpoints were prospectively selected. Values from one BAPN-treated mouse were not generated, when it was found after euthanasia that meniscectomy was not performed properly. Additionally, for LOX(L) activity in sera, one PBS-treated mouse was
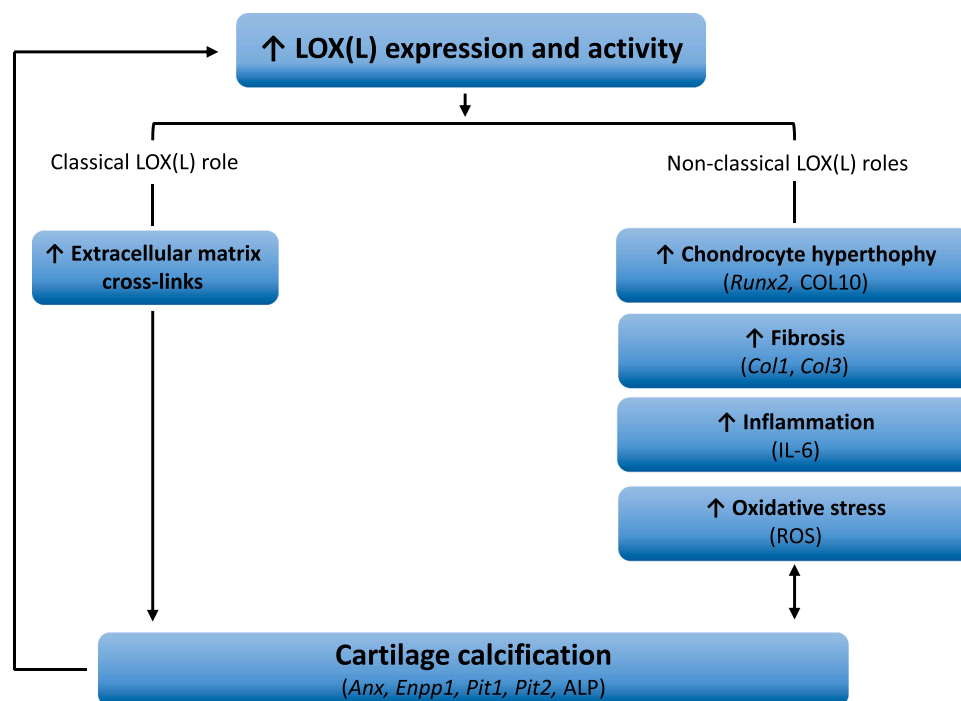
Fig. 6. Proposed mechanism based on the observed results. Increased LOX(L) expression and activity promotes cartilage calcification (*Anx, Enpp1, Pit1, Pit2,* ALP). Both classical LOX(L) role (matrix cross-links) and non-classical roles are involved. The latter encompass: increased chondrocyte hypertrophy (*Runx2,* COL10), increased fibrosis (*Col1, Col3*), increased inflammation (IL-6) and increased oxidative stress (ROS). Finally, cartilage calcification can in turn induce increased LOX(L) activity.

excluded as it was identified as an outlier by Grubb's test (p < 0.01). Given the cost and duration of the meniscectomy experiment, it was performed only once. Lastly, the concentrations of BAPN utilized in this manuscript were selected from prior publications and received approval from the Veterinary Authority before experimentation. For in vitro investigations, we consulted [38,39], and for in vivo studies, we were guided by [40–42].

4.2. Murine chondrocytes isolation and culture

Chondrocytes were isolated from 7-day old mice as previously described [14]. They were amplified in DMEM GlutaMAX with 10% FBS for 7 days. Different calcification media (CM) and control medium (Nt= not treated) were used, as specified below for each experimental setting. Media were refreshed every 3 days of culture.

4.3. Human chondrocytes isolation and culture

$$ LDH \quad release \quad (\%) = \frac{(value \quad in \quad sample) - (background)}{(Value \quad in \quad Triton \quad X100 treated \quad sample) - (background)} \quad x100 $$

Human primary chondrocytes were isolated from four OA patients undergoing knee replacement at Lausanne University Hospital, Switzerland (average age 73 ± 10, 2 females 2 males), as described previously [43]. Cells were amplified and cultured in DMEM GlutaMAX with 10% FBS for 21 days.

4.4. Calcification experiments

Chondrocytes were plated in monolayers at $5 * 10^4$ cells/cm², or in 3D micromasses obtained after centrifugation of $5 * 10^5$ cells. Cells were cultured for 14 days in CM= BGJb GlutaMAX medium (Gibco) supplemented with 10% FBS, 0.2 mM L-ascorbic acid 2-phosphate (Sigma), 20 mM β-glycerol phosphate (Sigma) and treated or not with 500 μM of the BAPN (Sigma). At the end of experiment, supernatants were removed for analyses, cell monolayer and micromasses were fixed. Crystal deposition was evaluated by Alizarin red staining. In monolayer it was quantified by dissolution of crystals in cetylpyridinium chloride [44], while in micromasses sections by image binarization and pixel counting in Adobe® Photoshop® (% of positive pixels over total number) of three or more independent fields.

4.5. Induction of joint calcification and BAPN treatment in mice

12 weeks old WT female mice in a C57BL/6 background were used. Mice were anesthetized via continuous isoflurane inhalation and knee joint instability induced surgically by partial medial meniscectomy (MNX) [45] of the right knee. The contralateral knee was sham operated as control. One group of mice (n = 10) was injected *i.p.* two times per week with 0.5 ml PBS. The other group (n = 10) was injected with 0.5 ml of 50 mg/Kg BAPN and given 1 mg/ml BAPN in drinking water. After two months, mice were sacrificed via CO_2 inhalation, knees dissected, fixed in 10% formalin for 7 days and analyzed by microCT-scan.

4.6. Mouse knee MicroCT-scan

Knee images were acquired using a MicroCT-scan system (MILabs, Utrecht, The Netherlands) with the following parameters: ultrafocus, 40 kV, 0.25 mA, 0.1° rotation step over 360°, 100 ms exposure time. Reconstruction was performed using Milabs Reconstruction software,

with 18 μm resolution. Analysis was performed with Imalytics Preclinical (Milabs, Aachen, Germany). A reference phantom with known hydroxyapatite crystal concentrations was used to perform voxel transformation into mg/cm³ of HA. Reconstructed scans were filtered with Gauss filter 1, and threshold for calcification was set at 300 mg/cm³. Bone volume (mm³) and crystal content (μg) quantifications were performed on new calcified deposits, along with bone volume of medial posterior meniscus, lateral meniscus and rotula. Bone mineral density (BMD, mg/cm³) and trabecular thickness (Tb.Th, mm) were measured in tibial subchondral bone.

4.7. Cytotoxicity (LDH)

Lactate dehydrogenase (LDH) in supernatants was measured using CytoTox-ONE™ Homogeneous Membrane Integrity Assay (Promega) according to the manufacturer's instructions. LDH release (%) was calculated by using the following formula:

4.8. RNA extraction, cDNA synthesis and qRT-PCR analysis

Chondrocytes were plated at $7 * 10^4$ cells/cm² and cultured for 7 days in Nt medium= DMEM GlutaMAX + 10%FBS or in CM= BGJb GlutaMAX medium (Gibco) supplemented with 10% FBS, 0.2 mM L-ascorbic acid 2-phosphate (Sigma), 20 mM β-glycerol phosphate (Sigma) and treated or not with 500 μM BAPN. RNA was extracted (RNA Clean & Concentrator5, Zymoresearch), reverse transcribed (Superscript II, Invitrogen), and quantitative Real Time PCR (qRT-PCR) with gene specific primers using the LightCycler480®system (Roche Applied Science) was performed (Table 1). Data were normalized against Gapdh reference gene, with fold induction of transcripts calculated against the indicated control.

Table 1
RT-qPCR gene primers used.

Gene	Forward primer (5′ → 3′)	Reverse primer (3′ → 5′)
Gapdh	CTC ATG ACC ACA GTC CAT GC	CAC ATT GGG GGT AGG AAC AC
Col2a1	ACA CTT TCC AAC CGC AGT CA	GGG AGG ACG GTT GGG TAT CA
Col10a1	AAA CGC CCA CAG GCA TAA AG	CAA CCC TGG CTC TCC TTG G
Sox9	AAG ACT CTG GGC AAG CTC TGG A	TTG TCC GTT CTT CAC CGA CTT CCT
Runx2	GGG AAC CAA GAA GGC ACA GA	TGG AGT GGA TGG ATG GGG AT
Col1a1	ATG TTC AGC TTT GTG GAC CTC	GCA GCT GAC TTC AGG GAT GT
Col3a1	TCC CCT GGA ATC TGT GAA TC	TGA GTC GAA TTG GGG AGA AT
Alpl	TTG TGC CAG AGA AAG AGA GAG	GTT TCA GGG CAT TTT TCA AGG T
Ank	TGT CAA CCT CTT CGT GTC CC	GAC AAA ACA GAG CGT CAG CG
Anx5	CCT CAC GAC TCT ACG ATG CC	AGC CTG GAA CAA TGC CTG AG
Enpp1	CTG GTT TTG TCA GTA TGT GTG CT	CTC ACC GCA CCT GAA TTT GTT
Pit1	CTC TCC GCT GCT TTC TGG TA	AGA GGT TGA TTC CGA TTG TGC
Pit2	AAA CGC TAA TGG CTG GGG AA	AAC CAG GAG GCG ACA ATC TT
Il-6	TCC AGT TGC CTT CTT GGG AC	GTG TAA TTA AGC CTC CGA CT
Lox	CAC TGC ACA CAC ACA GGG AT	TGT CCA AAC ACC AGG TAC GG
Loxl1	TAC CGA CCC AAC CAG AAT GG	GCT GTG GTA ATG TTG GTG ACA
Loxl2	GAC CTA CAA CCC CAA AGC CT	ACC AAG GGT TGC TCT GGC
Loxl3	TTC ACA GAA GCC ACA GGG TG	CAA CTG ATG CTC CAC CTC AAT
Loxl4	TGG CGT TGC CTG TAT GAA CA	GAT GCT GTG GTA GTG CCT GT

4.9. Immunohistochemical (IHC) analysis

Murine Collagen 10 (COL10) expression on micromasses paraffin sections was evaluated using an anti-COL10 rabbit polyclonal antibody (Genetex, GTX37732). Collagen 1 (COL1) and Collagen 3 (COL3) expression were evaluated using an anti-COL1 rabbit polyclonal antibody (Boster, PA2140–2) and an anti-COL3 rabbit polyclonal antibody (Origene, AP06517PU-N) respectively. COL1, COL3 and COL10 expression were quantified by pixel counting in Adobe® Photoshop® (% of positive pixels over total pixel number) of the total micromass area.

4.10. Two-steps culture experiment

In a first step we prepared matrices with different degrees of collagen cross-links by plating chondrocytes at $5 * 10^4$ cells/cm^2 and culturing them for 21 days in DMEM GlutaMAX with 10% FBS in presence or absence of BAPN (20, 100, 500 μM). After 21 days, cells were killed by overnight dry freezing at $-20\,^\circ$C and addition of 0.5% deoxycholate for 10 min at $4\,^\circ$C and extensively washed with PBS. In the second step, chondrocytes were plated on these differentially cross-linked matrices at $5 * 10^4$ cells/cm^2 and cultured for 3 days in CM= BGJb GlutaMAX medium (Gibco) supplemented with 10% FBS, 0.2 mM L-ascorbic acid 2-phosphate (Sigma), 20 mM β-glycerol phosphate (Sigma). At the end of the experiment, qPCR analysis was performed, and crystal deposition was assessed as described above.

4.11. Collagen content and collagen cross-links

Chondrocytes were plated at $5 * 10^4$ cells/cm^2 in T75 flasks for 21 days in CM= 3 mM high phosphate medium HPM ($NaH_2PO_4 \cdot H_2O$ + $Na_2HPO_4.2\,H_2O$) prepared in DMEM GlutaMAX low glucose (Gibco) supplemented with 10% FBS, 1x MEM Non-essential Amino Acids (MEM NEAA) (Sigma), 100 mM sodium pyruvate (Sigma) and 0.2 mM L-ascorbic acid 2-phosphate (Sigma). At the end of the experiment, supernatants were removed, monolayers washed in PBS, scraped and frozen at $-20\,^\circ$C. Collagen cross-links (DHLNL: dihydroxylysinonorleucine and HLNL: hydroxylysinonorleucine) were analyzed as previously described [46,47]. Collagen content was analyzed as previously described in [47], and collagen cross-links were normalized over it.

4.12. Alkaline phosphatase activity

Chondrocytes were plated at $7 * 10^4$ cells/cm^2, cultured for 7 days in CM= BGJb GlutaMAX medium (Gibco) supplemented with 10% FBS, 0.2 mM L-ascorbic acid 2-phosphate (Sigma), 20 mM β-glycerol phosphate (Sigma) and treated or not with 500 μM BAPN. Supernatant was removed and ALP activity was measured in cell lysate using a p-Nitrophenyl Phosphate assay (Abcam, ab83369), and normalized over protein content (Pierce™ BCA Protein Assay Kit). The manufacturer's protocols were explicitly followed, and absorbance was read at 405 nm at the Spectramax M5e plate reader.

4.13. LOX(L) activity

Chondrocytes were plated at $7 * 10^4$ cells/cm^2 and cultured for 24 h in CM= 3 mM HPM prepared in DMEM GlutaMAX no phenol red (Gibco) or CM= DMEM GlutaMAX no phenol red with secondary calciprotein particles (CPP, final concentration equivalent to 100 mg/ml calcium [21]). Alternatively, cells were stimulated with 500 μg/ml of pre-formed calcium-containing crystals (hydroxyapatite HA, octacalcium phosphate OCP and carbonated apatite CA) in DMEM GlutaMAX no phenol red. As control, cells were cultured in Nt medium= DMEM GlutaMAX no phenol red. LOX(L) activity was measured in chondrocytes supernatants and in cell lysates, by PromoKine Lysyl Oxidase Activity Assay Kit (PromoCell). Supernatant and lysate values were summed and normalized over protein content (Pierce™ BCA Protein Assay Kit).

4.14. Reactive oxygen species (ROS) measurement

Chondrocytes were plated at $5 * 10^4$ cells/cm^2 and cultured for 1 h in Nt medium=DMEM GlutaMAX no phenol red or in CM= 500 μg/ml HA crystals in DMEM GlutaMAX no phenol red. Concomitantly, cells were treated or not with 500 μM BAPN. Cellular ROS were measured by dihydroethidium (DHE, Life Technologies) and mitochondrial ROS were measured by MitoSOX (Life Technologies) following manufacturer protocols. Fluorescence was measured at 518/605 nm and 510/580 nm respectively using a spectrophotometer (Spectrax M5e, Molecular devices).

4.15. Bioinformatics analysis

First, the module containing LOX(L) family of enzymes (*Lox, Loxl1, Loxl2, Loxl3, Loxl4*) was identified as GO:0030199, namely collagen fibril organization module. Then, M-MAD (Modules by Module) selection was used in GeneBridge at www.systems-genetics.org/mmad [22]. Specifically, GO:0030199 was associated to calcification modules, hypertrophy modules and catabolic enzymes modules (Tables S1-S8). In the human data analysis, we chose 152 datasets from non-physiologically calcifying tissues, such as kidney, brain, skin, muscle, artery and soft tissues. In the murine data analysis, we chose 71 datasets from kidney, brain, skin and muscle. After tissue datasets selection, Manhattan plots were generated by the website.

4.16. Statistics

Plotted values represent means±SD. Data were analyzed with GraphPad Prism software (GraphPad software), San Diego, CA. Variation between data sets was evaluated using the Student's t-test or One-way or Two-way ANOVA test, where appropriate. Differences were considered statistically significant at $*p < 0.05$, $**\ p < 0.01$, $***\ p < 0.001$, $****\ p < 0.0001$.

4.17. Study approval

The studies involving human participants were reviewed and approved by the Centre Hospitalier Universitaire Vaudois, Lausanne, Switzerland. The patients provided their written informed consent to participate in this study. The animal study was reviewed and approved by the "Service de la Consommation et des Affaires Vétérinaires du canton de Vaud" Switzerland, animal authorization n° 3737. The animals care was in accordance with institutional guidelines.

CRediT authorship contribution statement

IB data curation, formal analysis, investigation, methodology; **EF** data curation, formal analysis; **MR** bioinformatics analysis; **JW** obtention of human cartilage samples; **JB** collagen cross-links analysis; **VC** data curation, formal analysis; **AS** writing review and editing; **TH** administration, resources, writing and editing; **NB** conceptualization, supervision, methodology, resources, validation, writing review and editing; **SN** conceptualization, data curation, formal analysis, funding acquisition, investigation, methodology, project administration, resources, supervision, validation, writing original draft and revision. SN and NB had access and verified all data.

Funding source

Declaration of Competing Interest

The authors declare that they have no known competing financial interests or personal relationships that could have appeared to influence the work reported in this paper.

Data Availability

All analyzed data are available in the main text or in the supplementary materials. All raw data are available upon request to the corresponding author.

Appendix A. Supporting information

Supplementary data associated with this article can be found in the online version at doi:10.1016/j.biopha.2023.116075.

References

[1] N. Yang, D.F. Cao, X.X. Yin, H.H. Zhou, X.Y. Mao, Lysyl oxidases: emerging biomarkers and therapeutic targets for various diseases, Biomed. Pharm. 131 (2020) 110791, https://doi.org/10.1016/j.biopha.2020.110791.

[2] M. Giampuzzi, et al., Lysyl oxidase activates the transcription activity of human collagene III promoter. Possible involvement of Ku antigen, J. Biol. Chem. 275 (2000) 36341–36349, https://doi.org/10.1074/jbc.M003362200.

[3] R. Oleggini, N. Gastaldo, A. Di Donato, Regulation of elastin promoter by lysyl oxidase and growth factors: cross control of lysyl oxidase on TGF-beta1 effects, Matrix Biol. 26 (2007) 494–505, https://doi.org/10.1016/j.matbio.2007.02.003.

[4] X.X. Nguyen, et al., Lysyl oxidase directly contributes to extracellular matrix production and fibrosis in systemic sclerosis, Am. J. Physiol. Lung Cell Mol. Physiol. 320 (2021) L29–L40, https://doi.org/10.1152/ajplung.00173.2020.

[5] S. Martinez-Revelles, et al., Lysyl oxidase induces vascular oxidative stress and contributes to arterial stiffness and abnormal elastin structure in hypertension: role of p38MAPK, Antioxid. Redox Signal 27 (2017) 379–397, https://doi.org/10.1089/ars.2016.6642.

[6] C. Meyers, et al., Heterotopic ossification: a comprehensive review, JBMR 3 (2019) e10172, https://doi.org/10.1002/jbm4.10172.

[7] M. Fuerst, et al., Calcification of articular cartilage in human osteoarthritis, Arthritis Rheum. 60 (2009) 2694–2703, https://doi.org/10.1002/art.24774.

[8] G.M. McCarthy, A. Dunne, Calcium crystal deposition diseases - beyond gout, Nat. Rev. Rheuma 14 (2018) 592–602, https://doi.org/10.1038/s41584-018-0078-5.

[9] S. Nasi, H.K. Ea, F. Liote, A. So, N. Busso, Sodium thiosulfate prevents chondrocyte mineralization and reduces the severity of murine osteoarthritis (https://doi.org:), PLoS One 11 (2016) e0158196, https://doi.org/10.1371/journal.pone.0158196.

[10] I. Bernabei, A. So, N. Busso, S. Nasi, Cartilage calcification in osteoarthritis: mechanisms and clinical relevance, Nat. Rev. Rheuma 19 (2023) 10–27, https://doi.org/10.1038/s41584-022-00875-4.

[11] G.D. Walker, M. Fischer, J. Gannon, R.C. Thompson Jr., T.R. Oegema Jr., Expression of type-X collagen in osteoarthritis, J. Orthop. Res 13 (1995) 4–12, https://doi.org/10.1002/jor.1100130104.

[12] P.M. van der Kraan, W.B. van den Berg, Chondrocyte hypertrophy and osteoarthritis: role in initiation and progression of cartilage degeneration? Osteoarthr. Cartil. 20 (2012) 223–232, https://doi.org/10.1016/j.joca.2011.12.003.

[13] J. Bertrand, et al., BCP crystals promote chondrocyte hypertrophic differentiation in OA cartilage by sequestering Wnt3a (https://doi.org:), Ann. Rheum. Dis. 79 (2020) 975–984, https://doi.org/10.1136/annrheumdis-2019-216648.

[14] S. Nasi, A. So, C. Combes, M. Daudon, N. Busso, Interleukin-6 and chondrocyte mineralisation act in tandem to promote experimental osteoarthritis, Ann. Rheum. Dis. 75 (2016) 1372–1379, https://doi.org/10.1136/annrheumdis-2015-207487.

[15] K. Morita, et al., Reactive oxygen species induce chondrocyte hypertrophy in endochondral ossification, J. Exp. Med 204 (2007) 1613–1623, https://doi.org/10.1084/jem.20062525.

[16] H.K. Ea, et al., Annexin 5 overexpression increased articular chondrocyte apoptosis induced by basic calcium phosphate crystals, Ann. Rheum. Dis. 67 (2008) 1617–1625, https://doi.org/10.1136/ard.2008.087718.

[17] J.H. Kim, et al., Matrix cross-linking-mediated mechanotransduction promotes posttraumatic osteoarthritis, Proc. Natl. Acad. Sci. USA 112 (2015) 9424–9429, https://doi.org/10.1073/pnas.1505700112.

[18] E.A. Makris, D.J. Responte, N.K. Paschos, J.C. Hu, K.A. Athanasiou, Developing functional musculoskeletal tissues through hypoxia and lysyl oxidase-induced collagen cross-linking, Proc. Natl. Acad. Sci. USA 111 (2014) E4832–E4841, https://doi.org/10.1073/pnas.1414271111.

[19] W. Alshenibr, et al., Anabolic role of lysyl oxidase like-2 in cartilage of knee and temporomandibular joints with osteoarthritis, Arthritis Res Ther. 19 (2017) 179, https://doi.org/10.1186/s13075-017-1388-8.

[20] M. Tashkandi, et al., Lysyl oxidase-Like 2 protects against progressive and aging related knee joint osteoarthritis in mice (https://doi.org:), Int J. Mol. Sci. 20 (2019), https://doi.org/10.3390/ijms20194798.

[21] P. Aghagolzadeh, et al., Hydrogen sulfide attenuates calcification of vascular smooth muscle cells via KEAP1/NRF2/NQO1 activation, Atherosclerosis 265 (2017) 78–86, https://doi.org/10.1016/j.atherosclerosis.2017.08.012.

[22] H. Li, et al., Identifying gene function and module connections by the integration of multispecies expression compendia, Genome Res 29 (2019) 2034–2045, https://doi.org/10.1101/gr.251983.119.

[23] M. Saito, K. Marumo, Collagen cross-links as a determinant of bone quality: a possible explanation for bone fragility in aging, osteoporosis, and diabetes mellitus, Osteoporos. Int 21 (2010) 195–214, https://doi.org/10.1007/s00198-009-1066-z.

[24] L. Knott, A.J. Bailey, Collagen cross-links in mineralizing tissues: a review of their chemistry, function, and clinical relevance, Bone 22 (1998) 181–187, https://doi.org/10.1016/s8756-3282(97)00279-2.

[25] E. Jover, et al., Inhibition of enzymes involved in collagen cross-linking reduces vascular smooth muscle cell calcification (https://doi.org:), FASEB J. 32 (2018) 4459–4469, https://doi.org/10.1096/fj.201700653R.

[26] K. Uto, S. Yoshizawa, C. Aoki, T. Nishikawa, H. Oda, Inhibition of extracellular matrix integrity attenuates the early phase of aortic medial calcification in a rodent model, Atherosclerosis 319 (2021) 10–20, https://doi.org/10.1016/j.atherosclerosis.2020.12.015.

[27] M.V. Bais, M.B. Goldring, LOXL2 as a protective in osteoarthritis cartilage, Aging (Albany NY) 9 (2017) 2024–2025, https://doi.org/10.18632/aging.101317.

[28] H. Iijima, et al., Age-related matrix stiffening epigenetically regulates alpha-Klotho expression and compromises chondrocyte integrity, Nat. Commun. 14 (2023) 18, https://doi.org/10.1038/s41467-022-35359-2.

[29] A.P. Singh, et al., alphaKlotho regulates age-associated vascular calcification and lifespan in zebrafish, 2767-2776 e2765, Cell Rep. 28 (2019), https://doi.org/10.1016/j.celrep.2019.08.013, 2767-2776 e2765.

[30] A. Santos, D. Lagares, Matrix stiffness: the conductor of organ fibrosis, Curr. Rheuma Rep. 20 (2018) 2, https://doi.org/10.1007/s11926-018-0710-z.

[31] P. Buttner, et al., Dissecting calcific aortic valve disease-the role, etiology, and drivers of valvular fibrosis (https://doi.org:), Front Cardiovasc Med 8 (2021) 660797, https://doi.org/10.3389/fcvm.2021.660797.

[32] V.E. Nava, R. Khosla, S. Shin, F.E. Mordini, B.C. Bandyopadhyay, Enhanced carbonic anhydrase expression with calcification and fibrosis in bronchial cartilage during COPD, Acta Histochem 124 (2022) 151834, https://doi.org/10.1016/j.acthis.2021.151834.

[33] A. Plaas, et al., The relationship between fibrogenic TGFbeta1 signaling in the joint and cartilage degradation in post-injury osteoarthritis. Osteoarthr. Cartil. 19 (2011) 1081–1090, https://doi.org/10.1016/j.joca.2011.05.003.

[34] F. Rodriguez-Pascual, T. Rosell-Garcia, The challenge of determining lysyl oxidase activity: Old methods and novel approaches, Anal. Biochem 639 (2022) 114508, https://doi.org/10.1016/j.ab.2021.114508.

[35] H. Sawada, Z.A. Beckner, S. Ito, A. Daugherty, H.S. Lu, beta-Aminopropionitrile-induced aortic aneurysm and dissection in mice, JVS Vasc. Sci. 3 (2022) 64–72, https://doi.org/10.1016/j.jvssci.2021.12.002.

[36] S.N. Cakir, L.E. de Castro Bras, Injury-specific inflammation leads to organ-specific fibrosis, Am. J. Physiol. Heart Circ. Physiol. 319 (2020) H610–H612, https://doi.org/10.1152/ajpheart.00598.2020.

[37] M.P. Vincenti, C.E. Brinckerhoff, Early response genes induced in chondrocytes stimulated with the inflammatory cytokine interleukin-1beta, Arthritis Res 3 (2001) 381–388, https://doi.org/10.1186/ar331.

[38] T. Ida, et al., Extracellular matrix with defective collagen cross-linking affects the differentiation of bone cells, PLoS One 13 (2018) e0204306, https://doi.org/10.1371/journal.pone.0204306.

[39] L. Shi, et al., Lysyl oxidase inhibition via beta-aminoproprionitrile hampers human umbilical vein endothelial cell angiogenesis and migration in vitro, Mol. Med Rep. 17 (2018) 5029–5036, https://doi.org/10.3892/mmr.2018.8508.

[40] A.J. Arem, R. Misiorowski, M. Chvapil, Effects of low-dose BAPN on wound healing, J. Surg. Res 27 (1979) 228–232, https://doi.org/10.1016/0022-4804(79)90134-3.

[41] L. Gao, et al., Effect of lysyl oxidase (LOX) on corpus cavernosum fibrosis caused by ischaemic priapism, J. Cell Mol. Med 22 (2018) 2018–2022, https://doi.org/10.1111/jcmm.13411.

[42] Y. Zheng, et al., Matrix stiffness triggers lipid metabolic cross-talk between tumor and stromal cells to mediate bevacizumab resistance in colorectal cancer liver metastases, Cancer Res 83 (2023) 3577–3592, https://doi.org/10.1158/0008-5472.CAN-23-0025.

[43] D. Ehirchiou, et al., CD11b signaling prevents chondrocyte mineralization and attenuates the severity of osteoarthritis, Front Cell Dev. Biol. 8 (2020) 611757, https://doi.org/10.3389/fcell.2020.611757.

[44] C.A. Gregory, W.G. Gunn, A. Peister, D.J. Prockop, An Alizarin red-based assay of mineralization by adherent cells in culture: comparison with cetylpyridinium chloride extraction, Anal. Biochem 329 (2004) 77–84, https://doi.org/10.1016/j.ab.2004.02.002.

[45] S. Kamekura, et al., Osteoarthritis development in novel experimental mouse models induced by knee joint instability (https://doi.org:), Osteoarthr. Cartil. 13 (2005) 632–641, https://doi.org/10.1016/j.joca.2005.03.004.

[46] J. Brinckmann, et al., Interleukin 4 and prolonged hypoxia induce a higher gene expression of lysyl hydroxylase 2 and an altered cross-link pattern: important pathogenetic steps in early and late stage of systemic scleroderma? Matrix Biol. 24 (2005) 459–468, https://doi.org/10.1016/j.matbio.2005.07.002.

[47] A.H. Nave, et al., Lysyl oxidases play a causal role in vascular remodeling in clinical and experimental pulmonary arterial hypertension, Arterioscler. Thromb. Vasc. Biol. 34 (2014) 1446–1458, https://doi.org/10.1161/ATVBAHA.114.303534.